VICTORIA UNIVERSITY
MELBOURNE AUSTRALIA

Effectiveness of vegetated patches as Green Infrastructure in mitigating Urban Heat Island effects during a heatwave event in the city of Melbourne

This is the In Press version of the following publication

The publisher's official version can be found at
https://www.sciencedirect.com/science/article/pii/S2212094718301981
Note that access to this version may require subscription.

Effectiveness of vegetated patches as Green Infrastructure in mitigating Urban Heat Island effects during a heatwave event in the city of Melbourne

H.M. Imran[a,c,d,*], J. Kala[b], A.W.M. Ng[a,d], S. Muthukumaran[a,d]

[a] College of Engineering and Science, Victoria University, Melbourne, Australia
[b] Environmental and Conservation Sciences, Murdoch University, Perth, Western Australia, Australia
[c] Institute of Water and Environment, Dhaka University of Engineering & Technology, Gazipur, Bangladesh
[d] Institute for Sustainable Industries & Livable Cities, Victoria University, Melbourne, Australia

ABSTRACT

The city of Melbourne in southeast Australia experiences frequent heatwaves and their frequency, intensity and duration are expected to increase in the future. In addition, Melbourne is the fastest growing city in Australia and experiencing rapid urban expansion. Heatwaves and urbanization contribute in intensifying the Urban Heat Island (UHI) effect, i.e., higher temperatures in urban areas as compared to surrounding rural areas. The combined effects of UHI and heatwaves have substantial impacts on the urban environment, meteorology and human health, and there is, therefore, a pressing need to investigate the effectiveness of different mitigation options. This study evaluates the effectiveness of urban vegetation patches such as mixed forest (MF), combination of mixed forest and grasslands (MFAG), and combination of mixed shrublands and grasslands (MSAG) in reducing UHI effects in the city of Melbourne during one of the most severe heatwave events. Simulations are carried out by using the Weather Research and Forecasting (WRF) model coupled with the Single Layer Urban Canopy Model (SLUCM). The fractions of vegetated patches per grid cell are increased by 20%, 30%, 40% and 50% using the mosaic method of the WRF model. Results show that by increasing fractions from 20 to 50%, MF reduces near surface (2 m) UHI (UHI_2) by 0.6–3.4 °C, MSAG by 0.4–3.0 °C, and MFAG by 0.6–3.7 °C during the night, but there was no cooling effect for near surface temperature during the hottest part of the day. The night-time cooling was driven by a reduction in storage heat. Vegetated patches partitioned more net radiation into latent heat flux via evapotranspiration, with little to no change in sensible heat flux, but rather, a reduction in the storage heat flux during the day. Since the UHI is driven by the release of stored heat during the night, the reduced storage heat flux results in reductions in the UHI. The reductions of the UHI_2 varied non-linearly with the increasing vegetated fractions, with lager fractions of up to 50% resulting in substantially larger reductions. MF and MFAG were more effective in reducing UHI_2 as compared to MSAG. Vegetated patches were not effective in improving HTC during the day, but a substantial improvement of HTC was obtained between the evening and early morning particularly at 2100 local time, when the thermal stress changes from strong to moderate. Although limited to a single heatwave event and city, this study highlights the maximum potential benefits of using vegetated patches in mitigating the UHI during heatwaves and the overall principles are applicable elsewhere.

1. Introduction

Urbanization results in increased runoff and decreased infiltration of water due to impervious surfaces. The higher thermal conductivity of construction materials in urban areas increases the absorption of solar radiation and reduced vegetation cover limits evapotranspiration. These changes in the surface energy balance can have impacts on near-surface air temperature, humidity, winds and atmospheric convection

(Liu et al., 2018; Morris et al., 2017). A well-documented impact of urbanization is the Urban Heat Island (UHI), defined as higher temperatures in city areas as compared to surrounding rural areas (Howard, 1833). In addition, the intensity of the UHI is amplified during heatwaves (Li et al., 2015; Zhao et al., 2018). From a meteorological context, a heatwave is usually defined as very unusual hot conditions for at least three consecutive days, during which the mean of minimum and maximum temperatures exceeds the climatological 95th percentile

(Nairn and Fawcett, 2013). The combination of UHI and heatwaves can severely affect urban meteorology, environment, energy demand and human health (Liu et al., 2018).

The higher temperatures in urban areas increases energy demand for cooling systems and water demand for urban landscape irrigation (Yu and Hien, 2006). The increased energy demand can also cause higher ambient temperatures via the use of air conditioners for building cooling systems (Ohashi et al., 2007). The UHI and heatwaves further amplify heat-related diseases and mortality (Mirzaei and Haghighat, 2010; Nicholls et al., 2008). For example, between 35,000 and 50,000 people are estimated to have died in Europe because of heat-related diseases during heatwaves in 2003 (Harlan et al., 2006). This threat is also important in Australia, with 374 and 167 additional human deaths during heatwaves in the state of Victoria in southeast Australia in 2009 and 2004 respectively (Victorian Auditor General's Report, 2014). The threats imposed by the UHI and heatwaves are very important in southeast Australia because of its hot summer, and these threats are likely to get worse in the future with projections that the intensity, frequency and duration of heatwaves in Australia will increase (Cowan et al., 2014).

The city of Melbourne, the capital of Victorian state of Australia, has been facing frequent heatwaves for the last two decades (Perkins-Kirkpatrick et al., 2016). For example, maximum temperatures of up to 45.1 °C and 43.9 °C were recorded in January 2009 and 2014 respectively (Victorian Auditor General's Report, 2014). In addition, the rate of urbanization is increasing rapidly to accommodate the increasing population. It is estimated that the population of the city of Melbourne will increase by 1.5–3.5 million by 2056 (Australian Bureau of Statistics, 2008). Hence, urban expansion will continue to meet the residential demands for the increasing population. Recently, the Victorian government released "Plan Melbourne 2050", a policy document which provides projections of future urbanization and recent studies have shown that this future urban expansion could increase the nocturnal near-surface UHI by 0.75–2.80 °C over the expanded urban areas during heatwaves in the city of Melbourne (Imran et al., 2018c). Therefore, impacts of the UHI, especially during heatwave events, must be minimized to make the city more resilient and livable.

A number of studies, including observational, modelling, or both, focusing on the micro to the meso-scale, have investigated the effectiveness of using different mitigation strategies to reduce the UHI in various cities. These strategies include increasing urban vegetation (Bowler et al., 2010; Coutts et al., 2016; Fallmann et al., 2013; Oliveira et al., 2011; Rizwan et al., 2008); use of water bodies (Hathway and Sharples, 2012; Theeuwes et al., 2013; Žuvela-Aloise et al., 2016) and changing the size and geometry of urban infrastructures (Ali-Toudert and Mayer, 2007; Middel et al., 2014). Adding more urban trees, parks, gardens, wetlands, and green roofs within urban areas, is generally referred to as the implementation of Green Infrastructure. The GI strategy is generally regarded as a sustainable strategy in mitigating UHI effects due to their multiple functionality and benefits for the urban environment such as increasing biodiversity and improving air quality in urban areas (Akbari et al., 2001). Initially, GI was defined as floodways, wetlands and parks, which provide water infiltration and flood control facilities (McMahon and Benedict, 2000). More recently, the definition has been expanded to include a variety of environmental and sustainability goals through a network of natural and planted vegetation such as street trees, parklands, rain gardens, community gardens, wetlands, green and cool roofs, and green walls (Foster et al., 2011). However, there is limited information about the potential of GI in mitigating UHI effects particularly during heatwaves when different GI scenarios are applied at the city scale. In addition, there is a pressing need to examine to what extent these mitigation strategies should be implemented to obtain substantial cooling benefits to mitigate UHI effects during heatwaves.

Increasing the areas of green spaces in urban areas can be an effective strategy to mitigate UHI effects by modifying the surface energy balance of the city by reducing storage heat in urban surfaces (Jacobs et al., 2018) and increasing evapotranspiration (Loughner et al., 2012). These two mechanisms play a key role in reducing UHI effects. Urban surfaces have higher thermal conductivity than vegetated surfaces, and store more heat during the day, which is later released at night. Hence, by decreasing the surface area of urban surfaces, and increasing the area of vegetated surfaces, storage heat is reduced during the day, leading to cooling at night. Another effect of vegetation on urban surfaces is direct shading by vegetation on urban surfaces, which also results in lower storage heat, and consequently, night-time cooling. Additionally, vegetated surfaces transform more of the net radiation to latent heat, rather than sensible heat, due to the evapotranspiration processes, and consequently, reduce urban temperatures. The size of green areas and their spacing play an important role in obtaining the optimum cooling benefit for the surrounding environment. Honjo and Takakura (1990) investigated the spatial extent of cooling effects of green areas based on their size. They reported that cooling effect extended to almost 300 m and 400 m, when the sizes of green areas were 100 m^2 and 400 m^2 respectively. Shashua-Bar and Hoffman (2000) used an empirical model to investigate the cooling effect of wooded sites using a combination of trees and urban green areas. They showed that the partially shaded areas by the tree canopy was the main driving factor for controlling air temperature within green areas, while tree characteristics and geometry played a limited role.

Urban vegetation also plays significant role in improving human thermal comfort within cities (Coutts et al., 2016; Shashua-Bar et al., 2010). Coutts et al. (2016) investigated the effects of street trees in reducing air temperature and improving Human Thermal Comfort (HTC) within individual streets at the micro-scale in the city of Melbourne in southeast Australia, and showed that urban trees are effective in reducing daytime Universal Thermal Climate Index (UTCI) during summer, whereby the thermal stress is reduced from very strong (UTCI > 38 °C) to strong (UTCI 32 °C). Furthermore, Jacobs et al. (2018) investigated the effectiveness of increasing urban vegetation, cool roofs and a combination of both strategies in reducing UHI effects and human thermal stress in the city of Melbourne using the Princeton Urban Canopy model (Wang et al., 2013) coupled with the WRF model. In their study, the percentage of urban grass was increased to evaluate the effectiveness of urban vegetation in reducing UHI intensity. Jacobs et al. (2018) report that urban vegetation is effective in mitigating UHI effects during the night due to lower ground/storage heat flux, with minimal cooling during the day, while cool roofs are more effective during the day but the combination of urban vegetation and cool roofs provides the maximum cooling benefit. Green and cool roofs have also been shown to reduce the UHI and improve the HTC particularly during the day, in the city of Melbourne during heatwaves (Imran et al., 2018a). Although all these studies provide highly valuable information on the effectiveness of different UHI mitigation strategies, the effects of implementing different GI components such as mixed forest, shrublands and grasslands, and their combined effects in reducing UHI effects and improving HTC for the city of Melbourne during heatwave events need further investigation. In addition, given the impacts of future urban expansion in Melbourne on the UHI (Imran et al., 2018c), there is a need to investigate the effectiveness of different GI components in reducing UHI impacts during heatwaves under future urban expansion scenarios. By implementing different types of urban vegetation/GI components, this study further builds on Imran et al. (2018c) by examining the effectiveness of different areas of vegetated patches within urban grid cells in reducing UHI effects due to urban expansion. The aim of this study is to evaluate the effectiveness of different types of urban vegetated patches, such as mixed forest, mixed forest with grasslands and mixed shrublands with grasslands in mitigating UHI effects and improving HTC at a city scale (meso-scale) during one of the most severe heatwave events, using the latest future urban expansion scenario for the city, as per the "Plan Melbourne 2050" urban expansion strategy. Simulations are carried out by increasing fractions of
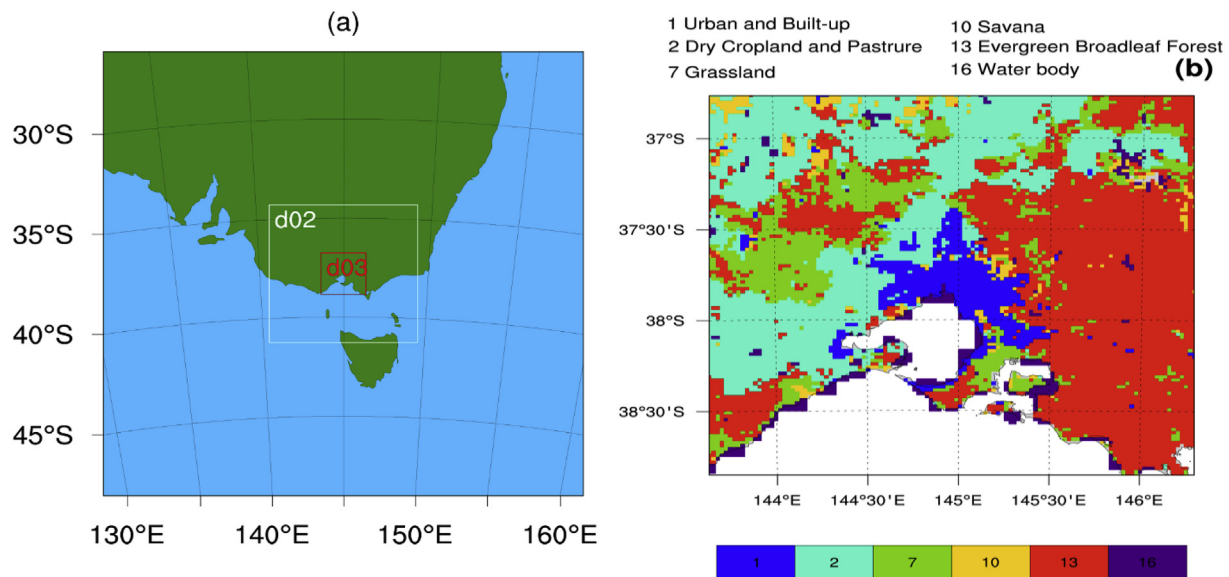
Fig. 1. (a) WRF domain configuration, where d02 and d03 represent second and innermost domains with resolution 6 km and 2 km, respectively, (b) Dominant land use classification in the innermost domain (d03) incorporating future urban expansion according to Plan Melbourne 2050.

vegetated patches within urban grid cells to investigate the maximum possible cooling benefits that can be obtained.

2. Methodology

2.1. Model configuration

Numerical weather and climate models are effective and commonly used in urban meteorology studies. One of the most widely used models is the Weather Research and Forecasting (WRF) model, which has been used in numerous urban meteorology studies (Li et al., 2014, 2015; Imran et al., 2018a; Jacobs et al., 2017, 2018; Liu et al., 2018; Morris et al., 2017; Sharma et al., 2016). This study uses the Weather Research and Forecasting (WRFv3.8.1) model with the Advanced Research WRF (ARW) dynamics solver (Skamarock et al., 2008).

The WRF model was operated using three nested domains (d01, d02 and d03) at 18, 6 and 2 km horizontal resolution respectively, as illustrated in Fig. 1a. The largest domain (d01) includes a larger part of southeast Australia and the second domain (d02) covers major part of Victorian State. The innermost domain covers the Melbourne metropolitan and surrounding rural areas. The dominant land use categories for each grid cell are derived from the 24-USGS land use classification. Furthermore, the urban grid cells were modified based on the Plan Melbourne 2050 urban expansion strategy (more details about plan Melbourne at http://www.planmelbourne.vic.gov.au/the-plan). Such re-classification of urban land use represents the future urban expansion for the city of Melbourne. Following Imran et al. (2018c) who investigated the impacts of future urbanization on the UHI during heatwaves in Melbourne, all urban expansion was set to high-density urban. This is also consistent with other studies, which have investigated the impacts of future urban expansion for other Australian cities (e.g., Argüeso et al., 2014). The dominant land use classification for the innermost domain are shown in Fig. 1b. 38 vertical levels were used (model top at 50 hPa), spaced closer together near the surface, and wider apart in the upper atmosphere. Initial and boundary conditions were from 6-hourly ERA-interim reanalysis, which has a spatial resolution of $0.75 \times 0.75°$ (Dee et al., 2011).

The WRF model offers a number of physics options for each physical parameterization including the Land Surface Model (LSM), Planetary Boundary Layer (PBL), cumulus parameterization, short and longwave radiation (SW and LW) and microphysics (MP), and the model is known

to be sensitive to selection of different physics options (e.g., Evans et al., 2012; Imran et al., 2018b; Kala et al., 2015a). This study uses the physics options suggested by Imran et al. (2018b), who conducted an extensive sensitivity analyses of the different physical parameterizations of the WRF model in simulating the UHI during heatwaves for the city of Melbourne, including the heatwave event in this study. By evaluating an ensemble of WRF simulations against station, gridded and sounding observations, Imran et al. (2018b) provide an ideal WRF set-up for simulating the UHI during heatwaves. This set-up has been used and further evaluated by Imran et al. (2018a), who investigated the effectiveness of green and cool roofs as UHI mitigation strategies during heatwaves in Melbourne. Hence this study uses the same set-up, which includes: unified Noah LSM (Chen and Dudhia, 2001), the Thompson MP scheme (Thompson et al., 2008), the Mellor-Yamada-Janjic PBL scheme (Janjic, 1994), the RRTMG SW and LW schemes (Iacono et al., 2008), the Monin-Obukhov similarity scheme for the surface-layer and the Grell–Devenyi scheme (Grell and Dévényi, 2002) scheme for cumulus convective parameterization. The cumulus scheme is only used for the two outermost domains d01 (18 km) and d02 (6 km) as the innermost domain, d03 (2 km) is at a sufficiently high resolution to resolve convection.

Additionally, WRF was operated with the unified Noah LSM coupled with the Single Layer Urban Canopy Model (SLUCM) (Chen and Dudhia, 2001; Chen et al., 2011; Liu et al., 2006) with the mosaic option. The SLUCM calculates fluxes for the urban surfaces within a grid cell, and incorporates parameterization of physical processes involved in the exchange of heat, momentum and water vapor in the urban environment by considering shadowing effects from buildings, reflection of shortwave and longwave radiation, wind profile in the canopy layer and a multilayer heat transfer equation for roofs, walls, and road surfaces (Kusaka and Kimura, 2004; Kusaka et al., 2001). On the other hand, the Noah LSM calculates fluxes for the vegetated portion of the grid cell. Thus, the coupled Noah-LSM and the SLUCM complete the urban surface energy balance by calculating fluxes from both the vegetated portion and built/impervious portion of urban areas. However, an important limitation of WRF-SLUCM is that the model does not resolve direct interactions between vegetation and urban surfaces, such as the shading effects of vegetation on buildings facades and roads, whereas more sophisticated urban canopy models resolve such effects (e.g., Lee and Park, 2008; Lemonsu et al., 2012; Krayenhoff et al., 2013; Redon et al., 2017). Since the aim of this paper is to investigate the

effects of relatively large portions of urban grid cells being completely converted to vegetation, rather than the implementation of vegetation within individual urban canyons, direct shading of urban surfaces by vegetation is not the key mechanism, and hence this limitation is reasonable given the aims. We note that we do not show any model evaluation in this paper since extensive model evaluation against observations for the same heatwave event, using the same WRF version and configuration has already been carried by Imran et al. (2018b), and additional model evaluation is also provided in Imran et al. (2018a). Both studies showed that WRF was able to simulate the UHI and heatwave conditions well.

The Noah LSM in WRF can be operated by using either dominant land-use types or a mosaic approach. When using dominant land-use types, the whole grid cell represents only one land use category. On the other hand, when mosaic approach is used, a grid cell can be subdivided into multiples tiles, to represent different land use categories within a single grid cell. This method is ideal to investigate the effects of converting relatively large portions of urban grid cells to vegetation. Moreover, recent studies by Sharma et al. (2017) have showed that use of the mosaic approach in WRF to represent sub-grid scale variations in land use improved simulation of the UHI for the city of Chicago in the USA. The mosaic approach allows a user to introduce different land use types into individual grid cells. To investigate the effectiveness of different vegetated patches in mitigating UHI effects, the mosaic approach was used, with two tiles per grid cell for MF and MSAG and three tiles per grid cell for MFAG (more details in section 2.2). When the mosaic approach is used, the SLUCM is used only for the urban tile instead of the whole grid cell, and the Noah LSM is used for the vegetated portion.

2.2. Numerical experiments

Following our recent work which examined the effectiveness of green and cool roofs in mitigating UHI effects in Melbourne during a heatwave event (Imran et al., 2018a), we focus on one of the most severe heatwave events, which occurred from the 27th to 30th January 2009. All simulations were conducted for four days and the first 24 h were considered as spin-up time, following our previous study (Imran et al., 2018a). This heatwave event occurred after a long of period of drought (Nicholls and Larsen, 2011), and antecedent soil moisture conditions played an important role (Kala et al., 2015b). To examine the effectiveness of different types of GI scenarios, a portion of each urban grid cell is replaced with different types of vegetated patches, namely, MF, MSAG and MFAG by using the Mosaic option. MF is a combination of different trees such as evergreen broadleaf/needleleaf trees and deciduous broadleaf/needleleaf trees. The city of Melbourne's urban forest strategy is that urban forest will be no more than 5% of any tree species, no more than 10% of any genus and no more than 20% of any one family (Melbourne (Vic.) Council, 2011). Therefore, this study uses the mixed type of vegetation, which includes mixed forest, shrublands and grasslands. To evaluate the potential city-scale effects of the proposed vegetated patches, comparisons are made between the control run (includes both current urban land use and future urban expansion) and experiments (includes different vegetated patches implemented into all urban grid cells). For all simulations, the urban and built areas are modified following Imran et al. (2018c) based on the Plan Melbourne 2050 urban expansion strategy and increasing fractions of each vegetated patch (Table 1) are incorporated into all urban grid cells (includes current urban and 2050 urban expansion). All these simulations were carried out by increasing the land-use fraction within all urban grid cells by 20%, 30%, 40% and 50%, as summarized in Table 1, and Table 2 summarizes key properties of the different plant functional types. It should be noted that urban surfaces in the SLUCM are assigned an urban fraction (Chen et al., 2011), e.g., 0.9 for high density urban as used in this study. The rest is assumed to be grass, and the minimum and maximum LAI for the urban category in Table 2 refers to the 0.1 grass fraction. The shade factors in Table 2 refer to direct

shading on the ground by the different vegetation types or urban grid cells. It is important to note that these shade factors do not represent shading of vegetation on urban surfaces and vice-versa as this is not resolved by the model.

2.3. Pedestrian level HTC calculation

Following Imran et al. (2018a) and Imran et al. (2018c), this study uses the Universal Thermal Comfort Index (UTCI) index in quantifying the pedestrian level (2 m) HTC, via the UTCI index. The UTCI index is used to assess how different vegetated patches improve the HTC in the city of Melbourne. The UTCI index calculates a physiological response based on meteorological and several human thermal parameters and represents human bioclimatic conditions and their relevance to human thermal stress. The UTCI index is used in representing human thermal stress under various climatic conditions (Blazejczyk et al., 2012; Vatani et al., 2016), which makes this index widely used. Temperature, relative humidity and solar radiation simulated by the WRF model were used as meteorological input and a default clothing factor of 0.90 and activity rate of 80 W for a male of 35 years are used as human thermal parameters. All these variables were used as input to the bioclimatic model RayMan Pro 3.1 (Matzarakis et al., 2007, 2010) to calculate the UTCI index. The HTC is classified as five categories based on the ranges of the UTCI index (Bröde et al., 2012) as shown in Table 3.

3. Results

3.1. Diurnal variations of the UHI

Before investigating the effects of different vegetated patches on the UHI, it is useful to first analyze the diurnal variation of the UHI from the control simulation to first understand its temporal evolution. Additionally, since the Plan Melbourne policy aims to increase vegetation cover by 40% by 2040, we also include results from 40% increase experiments. This is illustrated in Fig. 2, showing the hourly variation of the near surface (2 m) (UHI_2) and skin surface UHI (UHI_{sk}). The UHI_2 and UHI_{sk} are computed as the difference between urban and surrounding rural areas. The effectiveness of vegetated patches relative to urban areas in reducing the UHI_2 and UHI_{sk} is estimated as the difference of the UHI_2 and UHI_{sk}, respectively between the experiment (with different fractions of vegetated patches within urban grid cells) and control (only urban) ($UHI_{veg} - UHI_{urban}$). The control simulation shows the UHI_2 ranges from 1.0 to 5.9 °C and UHI_{sk} ranges from 2.0 to 11.0 °C. The UHI_2 and UHI_{sk} reach their peaks at 1900 and 2000 local time, respectively. The intensity of UHI_{sk} is higher than the UHI_2 especially between the evening and early morning. The intensity of UHI_{sk} is lower during the day as compared to the night, since the urban surfaces emit less heat during the day due to higher thermal conductivity of construction materials. On the other hand, urban surfaces re-radiate stored heat and result in higher skin-surface temperatures during the night. Vegetated patches reduce the UHI_2 and UHI_{sk} from evening to morning and no cooling effect is obtained during the day while the maximum UHI_2 and UHI_{sk} occurred at 1900 and 2000 local time, respectively.

3.2. Reductions of the UHI by different % of vegetated patches

Having examined the diurnal variation of the UHI_2 and UHI_{sk} from the control simulation and 40% experiments, we now examine the changes in the UHI_2 and UHI_{sk} with different percentages of vegetated patches within urban grid cells. This is illustrated in Fig. 3 showing the city-scale impacts of vegetated patches on the UHI_2 and UHI_{sk} averaged over three diurnal cycles from 28 to 30 January 2009 by using their fractions 20%, 30%, 40% and 50% (Table 1). The changes in UHI_2 and UHI_{sk} are calculated as the differences between the experiments and the control.

Fig. 3 Shows that MF was effective in reducing the UHI_2 and UHI_{sk}

Table 1
Design of numerical experiments for different vegetated patches.

Vegetated Patches	Urban Fraction (%)	Fraction of Vegetated Patch (%)	Combinations
Control (Urban)	100	–	Urban/Impervious areas
MF (Mixed Forest)	80	20	20% Mixed forest
	70	30	30% Mixed forest
	60	40	40% Mixed forest
	50	50	50% Mixed forest
MSAG (Mixed Shrublands and Grasslands)	80	20	20% Mixed shrublands and grasslands
	70	30	30% Mixed shrublands and grasslands
	60	40	40% Mixed shrublands and grasslands
	50	50	50% Mixed shrublands and grasslands
MFAG (Mixed Forest and Grasslands)	80	20	10% Mixed forest + 10% Grasslands
	70	30	15% Mixed forest + 15% Grasslands
	60	40	20% Mixed forest + 20% Grasslands
	50	50	25% Mixed forest + 25% Grasslands

from the night to morning (Fig. 3a–b). The UHI$_2$ shows smaller changes ($< 0.5\,°C$) as compared to UHI$_{sk}$. The reductions of UHI$_2$ and UHI$_{sk}$ increase with increasing fractions of MF. The UHI$_2$ reductions range from 0.6 to 3.4 °C during the night when the fraction of MF increases from 20% to 50% while the reductions of UHI$_{sk}$ range from 0.8 to 4.2 °C. Although the UHI$_{sk}$ increases slightly during the day (between 1000 and 1700 local time), there is no substantial increase in the UHI$_2$. Both the UHI$_2$ and UHI$_{sk}$ show maximum reductions at around 2100 local time. MSAG reduces the UHI$_2$ from 0.4 to 3.0 °C, and the UHI$_{sk}$ from 0.8 to 3.7 °C between the evening and early morning (Fig. 3c–d). It is noteworthy that MSAG shows more warming at the skin surface between 1000 and 1700 local time with an increase in the UHI$_{sk}$ between 0.3 and 1.0 °C, but there are no substantial changes in UHI$_2$. MFAG shows slightly higher effectiveness in reducing UHI effects during night as illustrated in Fig. 3e–f showing that increasing fractions of MFAG from 20 to 50% can reduce the UHI$_2$ by 0.6–3.7 °C, and UHI$_{sk}$ by 1.0–4.4 °C from evening to early morning. The maximum reduction occurs at 2100 local time, similar to the experiments with MF and MSAG.

Fig. 4 shows the relationship between reductions in the UHI$_2$ and UHI$_{sk}$ as a function of different vegetated fractions when the maximum UHI$_2$ and UHI$_{sk}$ reductions occurs at 2100 local time. There are non-linear relationships between the reductions of both UHI$_2$ and UHI$_{sk}$ and increasing vegetated fractions. Much larger reductions in the UHI$_2$ and UHI$_{sk}$ occur when vegetated fractions increases more than 40%. MFAG show the highest reductions in UHI$_2$ and UHI$_{sk}$ while the MSAG show the lowest reductions. The reductions of UHI$_2$ and UHI$_{sk}$ by MF are slightly lower as compared to MFAG.

3.3. Influence of different % of vegetated patches on the surface energy balance

To better understand the drivers of the changes in Figs. 3 and 4, we next examine the changes in the surface energy balance, as illustrated in Fig. 5 showing the sensible (SH), latent (LH) and ground (G) heat fluxes for the control and all experiments (Table 1). MF and MFAG do not show substantial changes in SH except for 50% MF and MFAG, which show reductions in SH between 20 and 40 W m^{-2} during midday as

Table 3
Universal Thermal Comfort Index (UTCI) range for different grades of human thermal perception and associated physiological stress (Bröde et al., 2012).

UTCI (°C)	Physiological Stress
+9 to +26	no thermal stress
+26 to +32	moderate heat stress
+32 to +38	strong heat stress
+38 to +46	very strong heat stress
> +46	extreme heat stress

compared to the control. Interestingly, all fractions of MSAG slightly increase SH (by approximately 10 W m^{-2}) during the day particularly at midday. By increasing vegetated fractions from 20 to 50%, LH increases by 20–120 for MF, 5 to 50 for MSAG and 20–130 W m^{-2} for MFAG during the day. It is noteworthy that the MF and MFAG show a higher increase in LH during the day as compared to MSAG. It is also noteworthy that there was a larger increase of LH for 20–30%, lower increase of LH for 30–40% and abruptly higher increase of LH for 50% vegetated patches. Storage heat decreases by 20–80 for MF, 20 to 60 for MSAG and 20–80 W m^{-2} for MFAG by increasing vegetated fractions from 20 to 50%. It should be noted that the increase in LH is not exactly balanced by the decrease in G and SH (e.g., for 50% MFAG). This is because G only includes the ground heat flux and not storage heat into building materials. All fractions of vegetated patches show a similar diurnal cycle of storage flux. A positive sign of storage heat during the night indicates heat fluxes flow from the surface to the atmosphere and vice-versa for negative storage heat during the day. The daytime reductions in storage heat flux are higher as compared to the nighttime reductions as less heat is stored during the day to be released during the night. The maximum reductions of storage heat occur at 1200 local time. MF and MFAG show higher reductions in storage heat and higher increases in LH as compared to MSAG. There were no substantial changes in net shortwave radiation but smaller reductions in net longwave radiation ranging from 5 to 15 W m^{-2} between late night and early morning (not shown). In summary, vegetated patches substantially alter the surface energy balance by increasing LH and

Table 2
Different properties of urban area and vegetated patches in the WRF model.

Urban/Vegetated Patches	Shade Factor	Minimum LAI	Maximum LAI	Minimum Albedo	Maximum Albedo
Urban	0.10	1.00	1.00	0.15	0.15
Mixed Forest (MF)	0.80	2.80	5.50	0.17	0.25
Mixed Shrubland/Grassland (MSAG)	0.70	0.60	2.60	0.22	0.30
Mixed Forest and Grassland (MFAG)	0.80	0.52	2.90	0.19	0.23

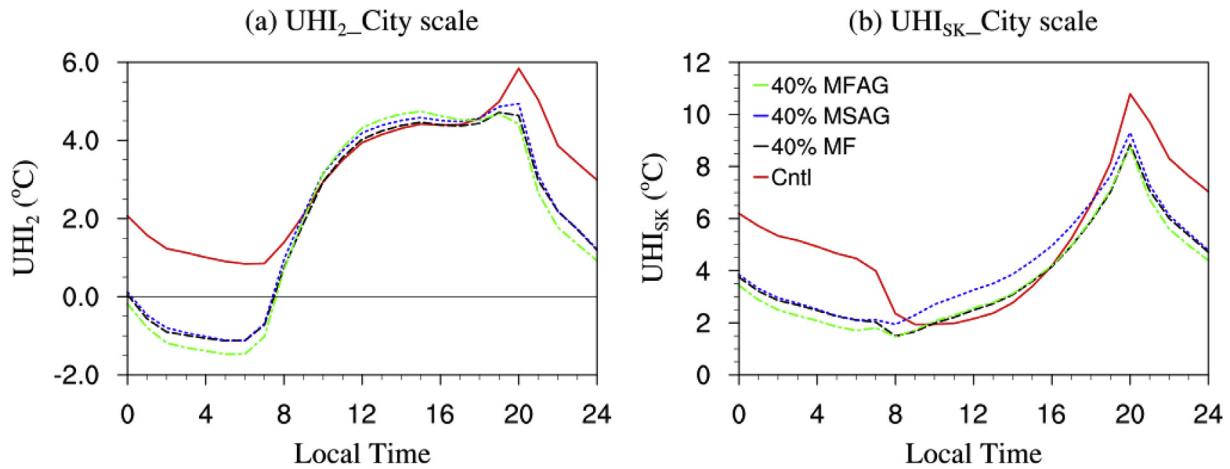## (a) UHI$_2$_City scale

(b) UHI$_{SK}$_City scale

Fig. 2. Diurnal variations of near surface (UHI$_2$) and skin-surface (UHI$_{sk}$) UHI averaged over the urban grid cells only across domain d03 over 3 days (28–30 January 2009), for the control simulation, and 40% MF, MSAG and MFAG experiments.

decreasing storage heat with relatively smaller changes in SH.

Fig. 3 showed that vegetated patches reduce the maximum UHI$_2$ and UHI$_{sk}$ at 2100 local time and this is related to reductions in storage heat during the day. By replacing part of an urban grid cell with vegetation, the storage heat flux is reduced, as urban surfaces have higher thermal conductivity than vegetated surfaces. Additionally, a higher proportion of vegetation in urban grid cells leads to partitioning of net radiation into LH due to evapotranspiration but there were no substantial reductions in SH. The reduced the storage heat in urban surfaces during the day which is released after sunset, leads to a cooling effect by the vegetated patches from evening to morning. On the contrary, MSAG show a slight warming effect during midday because of the slight increase in sensible flux at that time. Vegetated patches have little influence in reducing the UHI$_2$ during the day despite the fact that there is an increase in LH during this time. This is due to the fact that the increase in latent heat flux is not accompanied by a decrease in sensible heat flux, but rather changes in the ground heat flux. With little to no change in sensible heat flux, there are little to no changes in temperature during the day.

3.4. Spatial changes due to different vegetated patches

Having examined changes averaged over urban grid cells, we now examine the spatial changes across the domain. This is illustrated in Fig. 6 showing the spatial changes (experiments minus control) in mean T$_2$ when maximum reductions in the UHI occur (averaged from 2100 to 0400 local time from 28 to 30 January 2009) as a function of increasing fractions of vegetated patches. By increasing vegetated fractions from 20 to 50%, reductions in T$_2$ range from 0.5 to 5.0 °C for MF, 0.5 and 4.5 °C for MSAG, and 0.5–5.5 °C for MFAG. It is noteworthy that although the reduction ranges of mean T$_2$ are nearly similar for MF and MSAG, MFAG show higher reductions over larger areas. The highest reduction in the T$_2$ occurs in the center of the city. The non-linearity of the reduction in temperature with increasing fractions of vegetated patches shown earlier in Fig. 4 is further reflected in Fig. 6 showing the much larger reductions with 50% scenarios as compared to lower percentages.

Fig. 7 shows the changes in storage heat for increasing proportions of different vegetated patches averaged over the same period used for Fig. 6. The reductions in storage heat ranges from 5 to 35 W m^{-2} by increasing the fractions from 20 to 50% of MF and MSAG while the decrease in storage heat ranges from 5 to 40 W m^{-2} for MFAG by increasing the same fractions. MFAG and MF are slightly more effective in reducing the storage heat over larger areas as compared to MSAG.

The effects of the vegetated patches on the spatial distribution of

relative humidity (2 m) and wind speed (10 m) are shown in Figs. 8 and 9 respectively, averaged over the same period used for Fig. 6. The 20% MF, MSAG and MFAG experiments do not substantially increase the relative humidity as there are no substantial reductions of T$_2$ (Fig. 6). Increasing the fractions of vegetated patches from 30 to 40%, leads to increases in relative humidity by 2–8% for MF, MSAG and MFAG. The 50% MF, MSAG and MFAG experiments show substantial increases in relative humidity ranging from 4 to 14% because of larger reductions in T$_2$ (Fig. 6). The increases in relative humidity by MF and MFAG are higher as compared to MSAG. 50% vegetated patches lead to the highest increase in relative humidity over the urban areas as compared to other fractions. The increase in relative humidity is a direct result of the changes in temperature as where were no changes in mixing ratio. There were no substantial changes in relative humidity during the day (from 1100 to 1400 local time, not shown), when vegetated patches caused a slight warming effect.

Fig. 9 shows the changes in wind speed (experiments minus control) due to implementation of different fractions of vegetated patches in the urban areas. The wind direction from the experiments is overlaid on the changes in wind speed, as there were no substantial changes in wind direction due to the implementation of vegetated patches. Wind speed ranges between 5 and 7 m s^{-1} over urban areas for control experiment (not shown). The reductions in wind speed range from 0.25 to 1.25 m s^{-1} by increasing fractions of vegetated patches from 20 to 50%.

Furthermore, changes in the boundary layer structure, e.g., vertical profiles of air temperatures, wind speed, relative humidity, vertical wind component and turbulent kinetic energy were examined, but these did not show substantial changes and are therefore not shown. Vegetated patches did not substantially influence vertical mixing within the boundary layer during the heatwave event.

3.5. Changes in human thermal comfort (HTC)

Fig. 10 shows the HTC via the UTCI index for the control simulation (Fig. 10 (a)) and the changes in HTC for 40% (Fig. 10b) and 50% (Fig. 10c) vegetated patches as these vegetated fractions showed the largest changes in UHI$_2$ and UHI$_{sk}$. A lower UTCI index indicates higher HTC and vice-versa. The results illustrate that increasing vegetated patches in urban areas improves the HTC from evening to night in the urban areas. MF and MFAG increase HTC by reducing the UTCI index from 3.2 to 4.8 °C during the night by using 40–50% vegetated patches, while MSAG reduces UTCI index from 1.7 to 2.5 °C. The maximum improvement in HTC occurs during the evening (2100 local time), when the maximum UHI$_2$ and UHI$_{sk}$ reductions occur. No substantial improvement of HTC is obtained during the day (between 1000 and
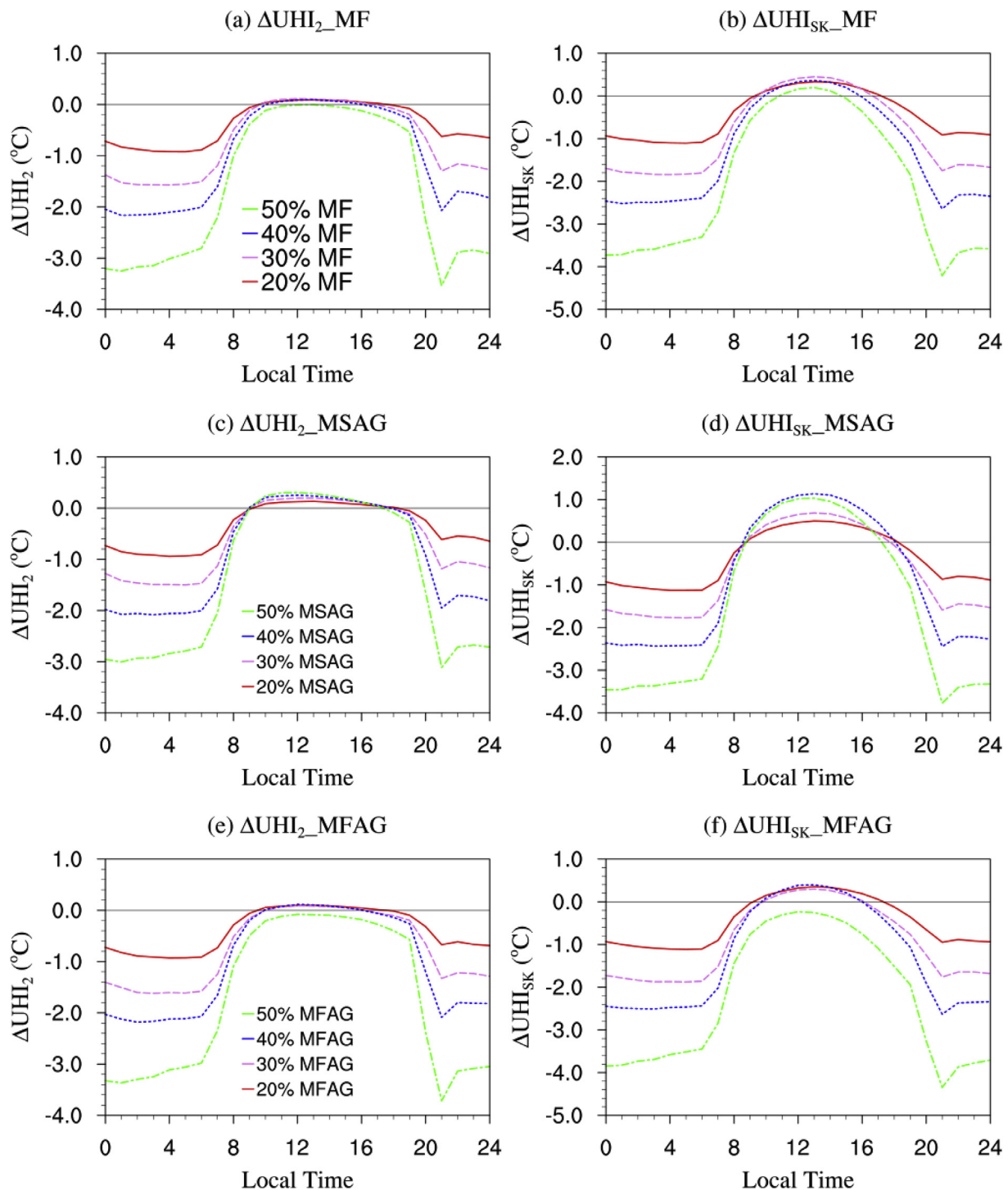
Fig. 3. Hourly changes (experiment minus control) in UHI_2 (left column) and UHI_{sk} (right column) for (a) and (b) MF, (c) and (d) MSAG and (e) and (f) MFAG by using their fractions 20%, 30%, 40% and 50%. The UHI_2 and UHI_{sk} have been averaged over urban grid cells only over 3 days from 28 to 30 January 2009.

1700 local time) especially when very strong human discomfort occurs. Therefore, vegetated patches are not able to improve HTC when stronger heat stress occurs. In addition, MSAG slightly deteriorate the HTC by increasing the UTCI index by 0.50 °C due to slightly higher sensible heat flux during the day (Fig. 10b and c). MF and MFAG show similar effectiveness in improving HTC (reducing UTCI) while MSAG show lower effectiveness as compared to MF and MFAG.

4. Discussion

This study examined the potential of different vegetated patches in urban areas in reducing UHI effects due to future urban expansion in the city of Melbourne during an extreme heatwave event. Although MF, MFAG and MSAG substantially increased latent heat flux and decreased storage heat during the day (Fig. 5), no substantial reductions of the UHI_2 and UHI_{sk} occurred during the day, as there was little to no change in sensible heat flux (Fig. 3). Rather there was a slight warming effect in the skin surface temperature between 1000 and 1700 local
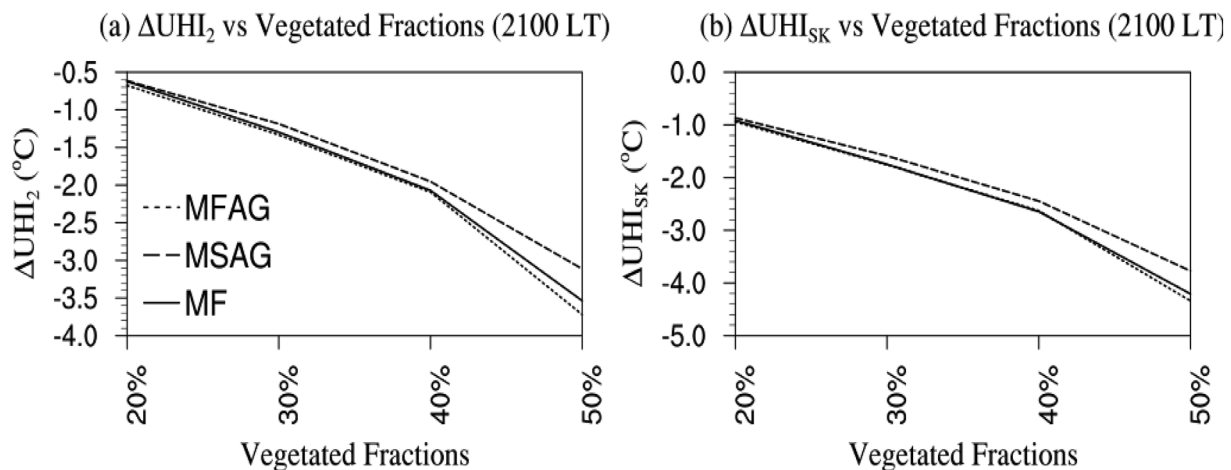
Fig. 4. Change in (a) UHI$_2$ and (b) UHI$_{sk}$ as a function of % vegetated patches when the reductions reach their maxima (2100 local time). The UHI$_2$ and UHI$_{sk}$ have been averaged over 3 days from 28 to 30 January 2009.

time which is likely due to the rapid release of terrestrial radiation and trapping of solar heat from MSAG, MFAG and MF as compared to a slower release from the urban surfaces as reported by Papangelis et al. (2012), who found similar warming effects over open vegetated urban green surfaces due to faster release of terrestrial radiation. Additionally, the heatwave event considered in this study resulted in very hot and dry conditions, and therefore, vegetated surfaces would like have become warmer as compared to usual summer days during the day. The key driver in substantial reduction of the UHI$_2$ and UHI$_{sk}$ between evening and early morning was the storage heat flux, and this result is consistent with Jacobs et al. (2018). The higher the reductions of storage heat (Fig. 7), the higher the reductions of the UHI$_2$ and UHI$_{sk}$ (Fig. 6). The main driver of the reduction in storage heat was the lower urban fraction with increasing fractions of vegetated patch implementation
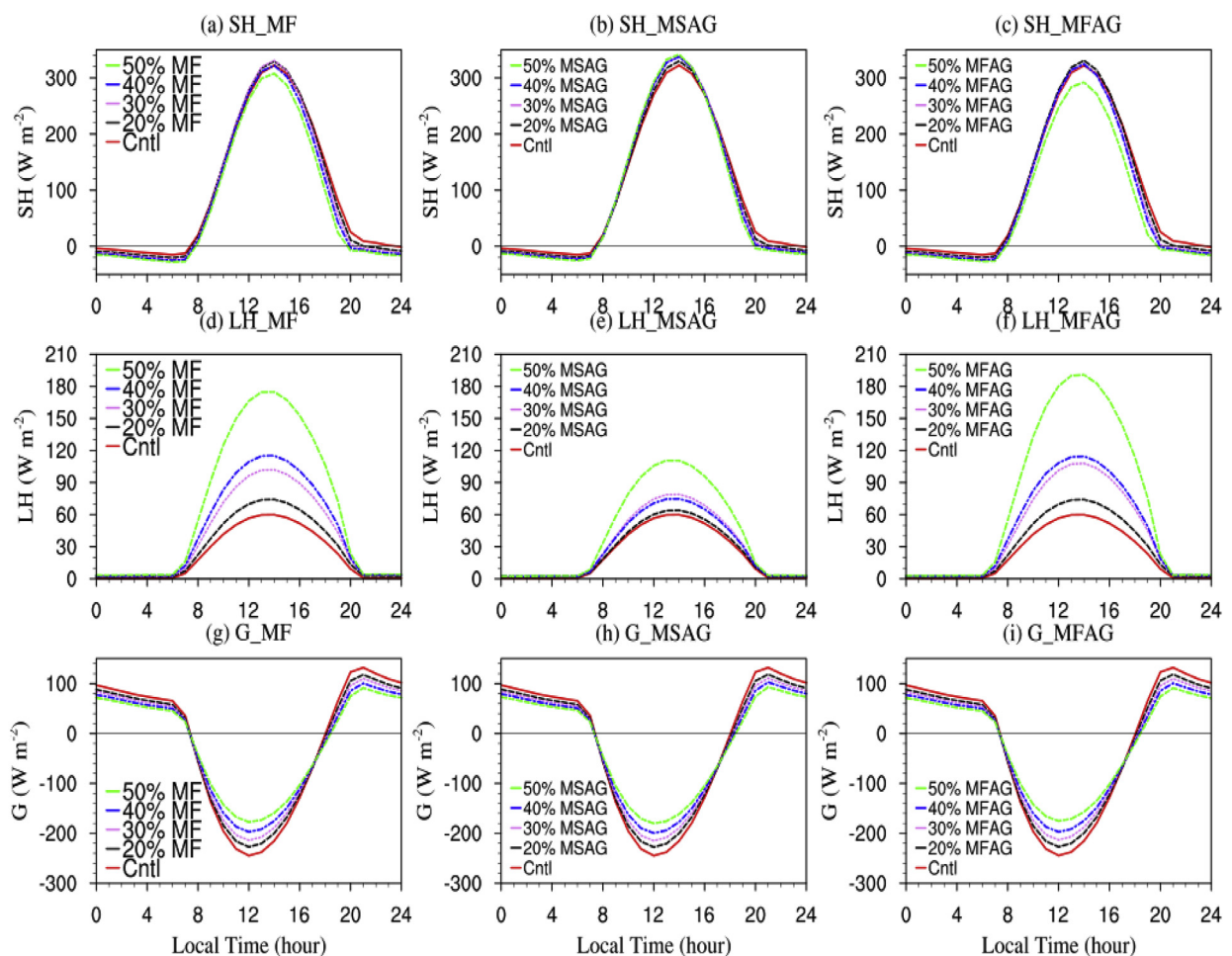

Fig. 5. Surface energy balance for MF (left column), MSAG (middle column) and MFAG (right column) for all experiments including the control simulation (Table 1), averaged over urban grid cells only in d03 (Fig. 1) over 3 days from 28 to 30 January 2009.
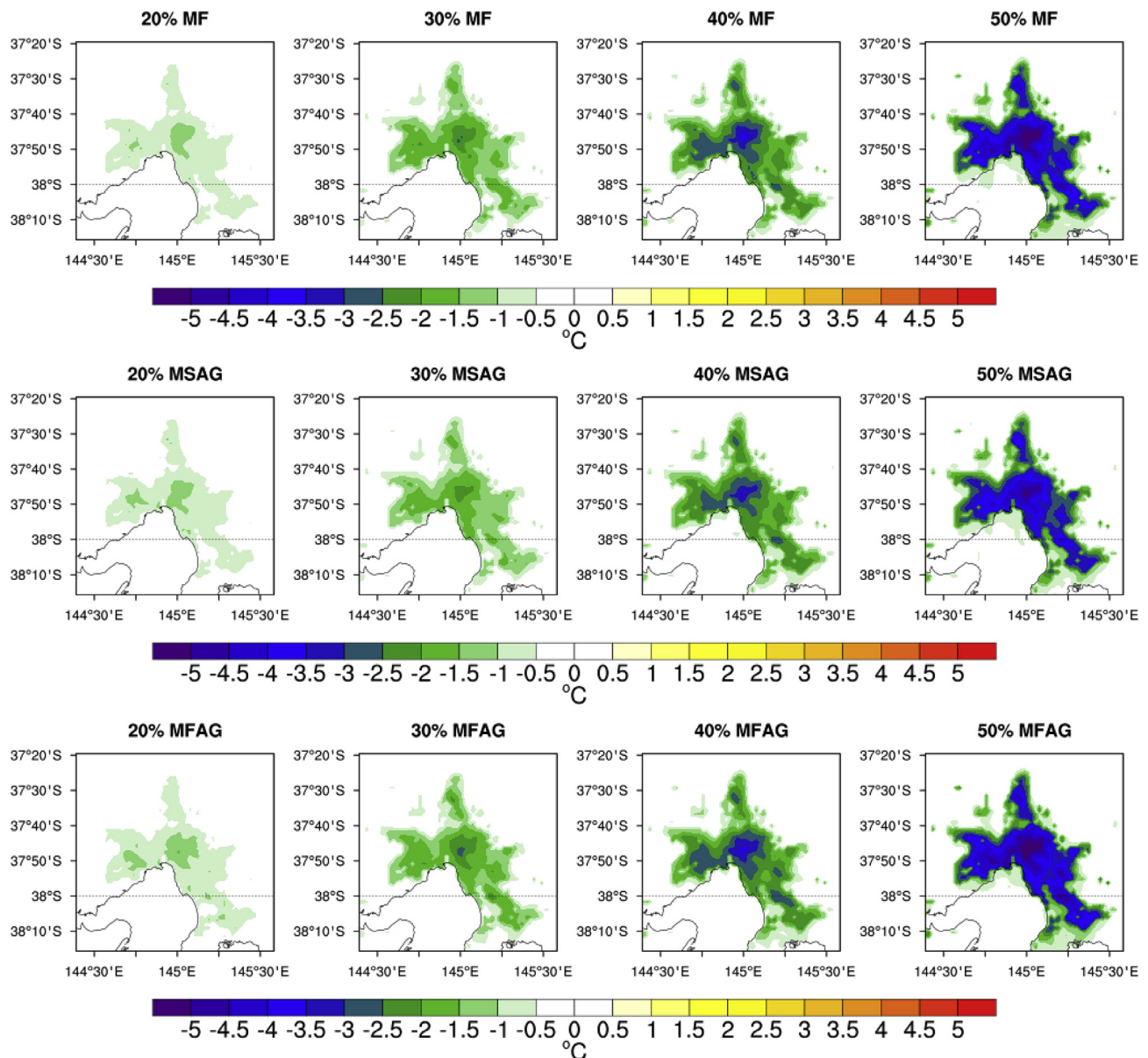
Fig. 6. Changes in T_2 (experiment minus control) by using 20%, 30%, 40% and 50% vegetated patches averaged from 2100 to 0400 (when maximum UHI_2 reduction occurs) local time over 3 days from 28 to 31 January 2009.

(Table 1).

A number of studies report daytime cooling of the near surface air temperature by increasing urban vegetation (e.g., Lee and Park, 2008; Loughner et al., 2012; Coutts et al., 2016) due to shading and evapotranspiration, but this study found no such cooling during the day. The urban canopy models and experiments used for those studies considered shading effects of urban vegetation over buildings, roads and walls, which was the main driving mechanism in reducing day time temperatures in urban areas. In this study, vegetation is implemented as patches using the mosaic approach, i.e., entire portions of urban grid cells are converted to vegetated surfaces, rather than the implementation of vegetation which urban canyons whereby the shading effect of individual trees on buildings would be a key factor. The nighttime cooling was driven by a reduction in storage heat by the urban surfaces during the day as the higher fractions of urban areas were replaced by vegetated surfaces (e.g., MF, MFAG and MSAG). MF and MFAG showed higher cooling effect as compared to MSAG since MF and MFAG had a lower storage heat. This lower storage heat is likely due to the to higher shade factor and LAI as compared to MSAG, which would have led to

even less radiation reaching the ground surface during the day, leading to lower storage heat. Similar findings have been reported by other studies (Kumar and Kaushik, 2005; Lin and Lin, 2010). Several studies have shown that leaf color (e.g., light green leaves) and LAI of plants are the most important factors in driving the cooling effect (Kumar and Kaushik, 2005; Lin and Lin, 2010; Rey, 1999; Tanaka and Hashimoto, 2006), with light-green leaves being more effective in reflecting solar radiation as compared to darker-green leaves and higher LAI of plants provides more cooling benefits via evapotranspiration. This study suggests that higher LAI and shade factor (on the ground) for MF and MFAG as compared to MSAG (Table 2) leads to higher reductions of the UHI_2 and UHI_{sk}. Although, the cooling effect of MF, MFAG and MSAG depend on other factors (e.g., leaf thickness, texture of trees), which are beyond the scope of this study. There was a slight warming effect at skin-surface level due to increasing vegetated patches particularly for MSAG at 1200 local time because of a slight increase in sensible heat. MSAG resulted in higher SH flux due their lower LAI and shade factor (Table 2) as compared to MF and MFAG. Lower LAI would have allowed more solar radiation to reach the surface, and given the very dry soil
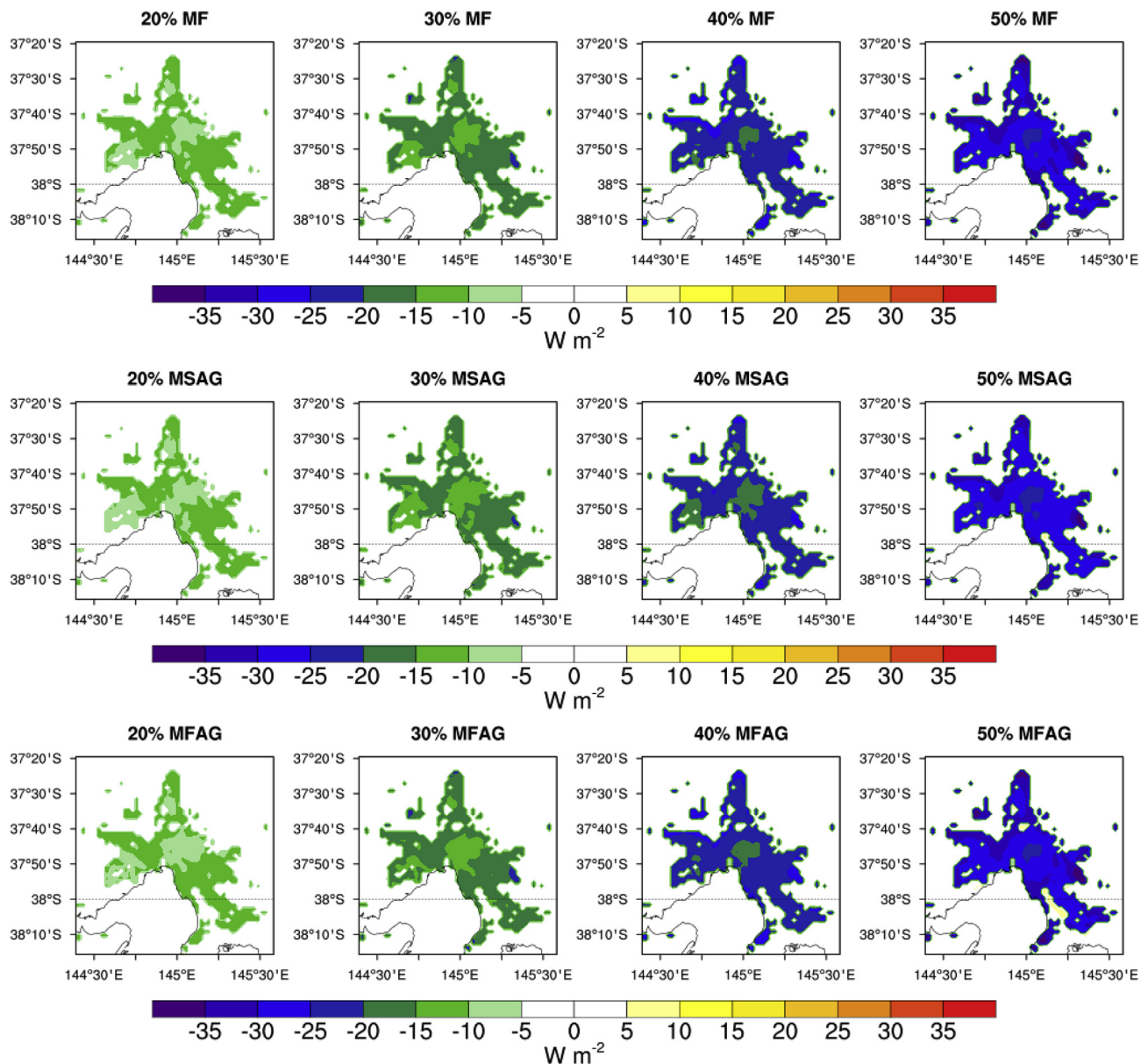
Fig. 7. Changes in storage heat (experiment minus control) for MF (upper), MSAG (middle) and MFAG (bottom) by using fractions 20%, 30%, 40% and 50%. All the results are averaged from 2100 to 0400 local time for the 3 days (28–30 January 2009) when maximum UHI$_2$ reductions occurred.

conditions during the heatwave, more solar radiation reaching the surface would have enhanced SH, and consequently led to a slight warming effect on skin surface temperature. Furthermore, increased vegetation patches showed minimal cooling effect for near surface temperature during the hottest part of the day similar to Jacobs et al. (2018).

Although previous studies showed that the cooling effect of parks extended to surrounding built-up areas (Papangelis et al., 2012; Yu and Hien, 2006) due to cooler air advection over the parks and downwind into the urban areas (Papangelis et al., 2012), this study did not show noticeable cooling effects beyond urban areas when different types of vegetated patches were used (Fig. 6). The reason was likely due to very dry air flowing from heated interior during the heatwave event, which limited cooling effects to surrounding areas. The relationship between the UHI reductions and increased fractions of vegetated patches was non-linear, with 50% vegetated patches resulting in much larger cooling benefits than lower fractions. This was most likely due to the reductions of wind speeds (Fig. 9) for 50% as compared to other vegetated fractions. The higher vegetated fractions led to weaker winds

particularly in the center of the city. These weaker winds would have promoted stagnation rather than advection of the cooler air, leading to more cooling in the city center (Fig. 6), where the reductions of wind speeds were higher (Fig. 9). Furthermore, MF and MFAG showed higher effectiveness in reducing UHI effects as compared to MSAG (Fig. 6) because of lower storage heat (Fig. 7), which is likely due to the higher shade factor and LAI (Table 2).

Earlier studies have shown that MFAG can result in reductions of air temperature by 5 °C in the city of Washington and Baltimore, USA (Loughner et al., 2012), and 2.5 °C due to MF in Athens, Greece (Papangelis et al., 2012) during the night, due to lower storage heat in the areas of MFAG and trees during the day and unobstructed and rapid release of this stored heat during the night. Loughner et al. (2012) showed that MFAG reduced neighborhood air temperature by 1 °C during the day because of advection of cooler air due to sea-breeze while Papangelis et al. (2012) reported the reduction of maximum day time temperature by 4.1 °C for MF due to the combined effects of tree shading and evapotranspiration, and sea-breeze. Although this study showed cooling benefits from different vegetated patches during the
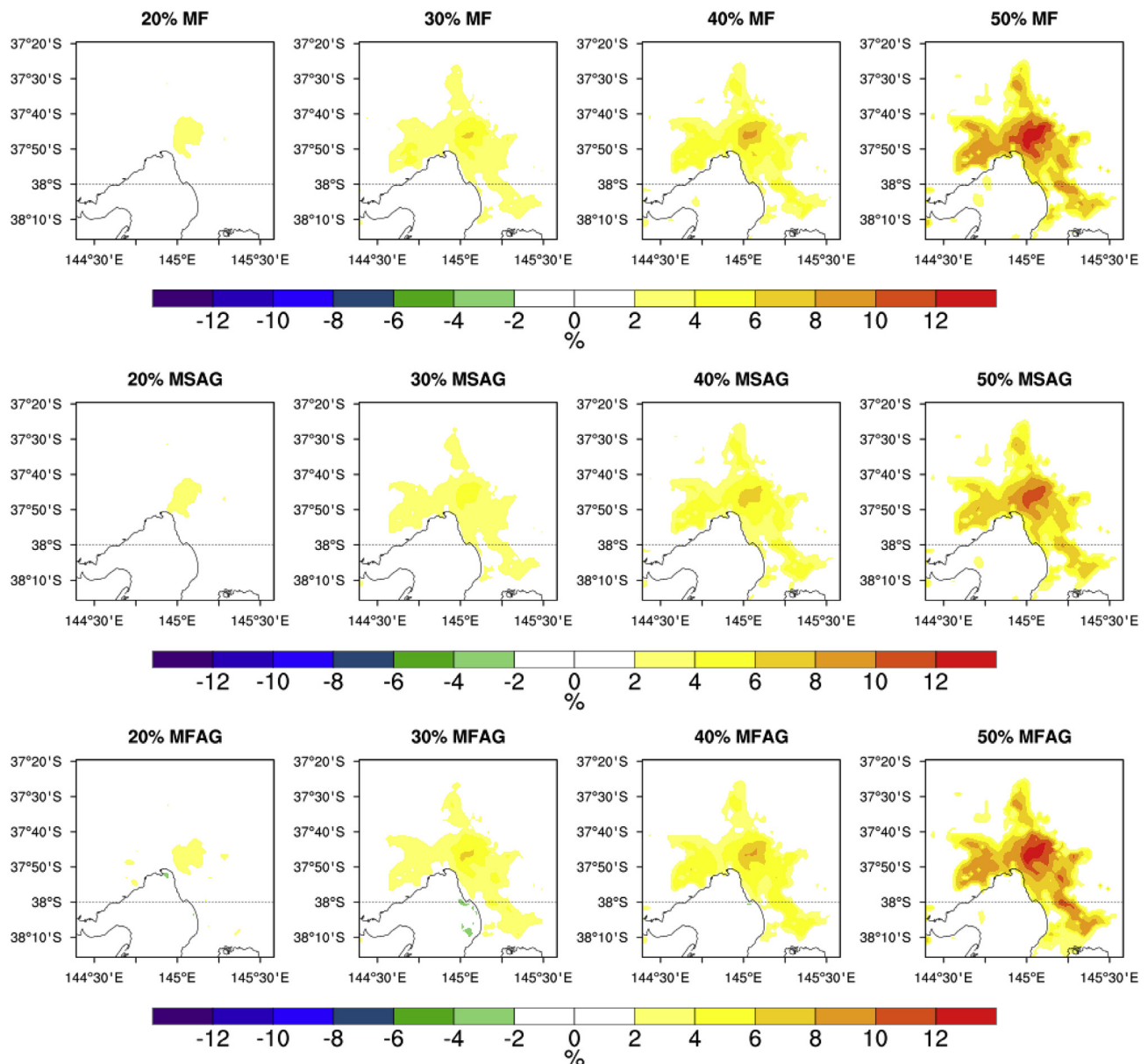
Fig. 8. Changes in relative humidity (experiment minus control) for MF (upper), MSAG (middle) and MFAG (bottom) by using fractions 20%, 30%, 40% and 50%. All the results are averaged from 2100 to 0400 local time for the 3 days (28–30 January 2009) when maximum UHI$_2$ reductions occurred.

night, there were no cooling effects during the day as no substantial reductions in SH occurred during this time.

Several studies have shown that changes in wind speed and direction were another driver in influencing the variability of air temperature as these variables play important role in influencing vertical mixing (Lin and Lin, 2010; Loughner et al., 2012; Park et al., 2012). This study did not show substantial reductions in wind speed for 20 and 30% vegetated patches (Fig. 9). However, the moderate reductions of wind speed (ranging from 0.50 to 1.25 m s^{-1}), particularly in the center of the city for 40 and 50% vegetated patches, could have had an influence on cooling in the center of the city. Vegetated patches were not effective in improving HTC during the day and the reason was most likely due to increased relative humidity during the same time (Fig. 10). However, HTC substantially improved during the night due to vegetated patches because of the reductions of storage heat (Figs. 5 and 7).

5. Conclusions

The study investigated the effectiveness of MF, MSAG and MFAG as

vegetated patches in reducing UHI effects in the city of Melbourne in southeast Australia using the mesoscale WRF model coupled with the SLUCM during a severe heatwave event. A future urbanization scenario was implemented based on the Plan Melbourne 2050 urban expansion strategy. Experiments were carried out by increasing the percentage of vegetated patches from 20 to 50% within all urban grid cells by using the mosaic approach in WRF. All vegetated patches led to reductions in the UHI$_2$ and UHI$_{sk}$ and thereby improved HTC from evening to early morning. The reductions of UHI$_2$ and UHI$_{sk}$ were higher when the fractions of vegetated patches were increased, but substantially higher when 50% was used, and the cooling effects were more intense in the center of the city. The application of different vegetated patches substantially altered the surface energy balance by substantially reducing storage heat and increasing latent heat flux, with the storage heat flux being the key driver in reducing UHI effects.

MF and MFAG were more effective in reducing UHI effects as compared to MSAG. On the other hand, MSAG resulted in slight warming during midday because of increased sensible heat flux due to lower LAI and shade factor. The effectiveness of different vegetated
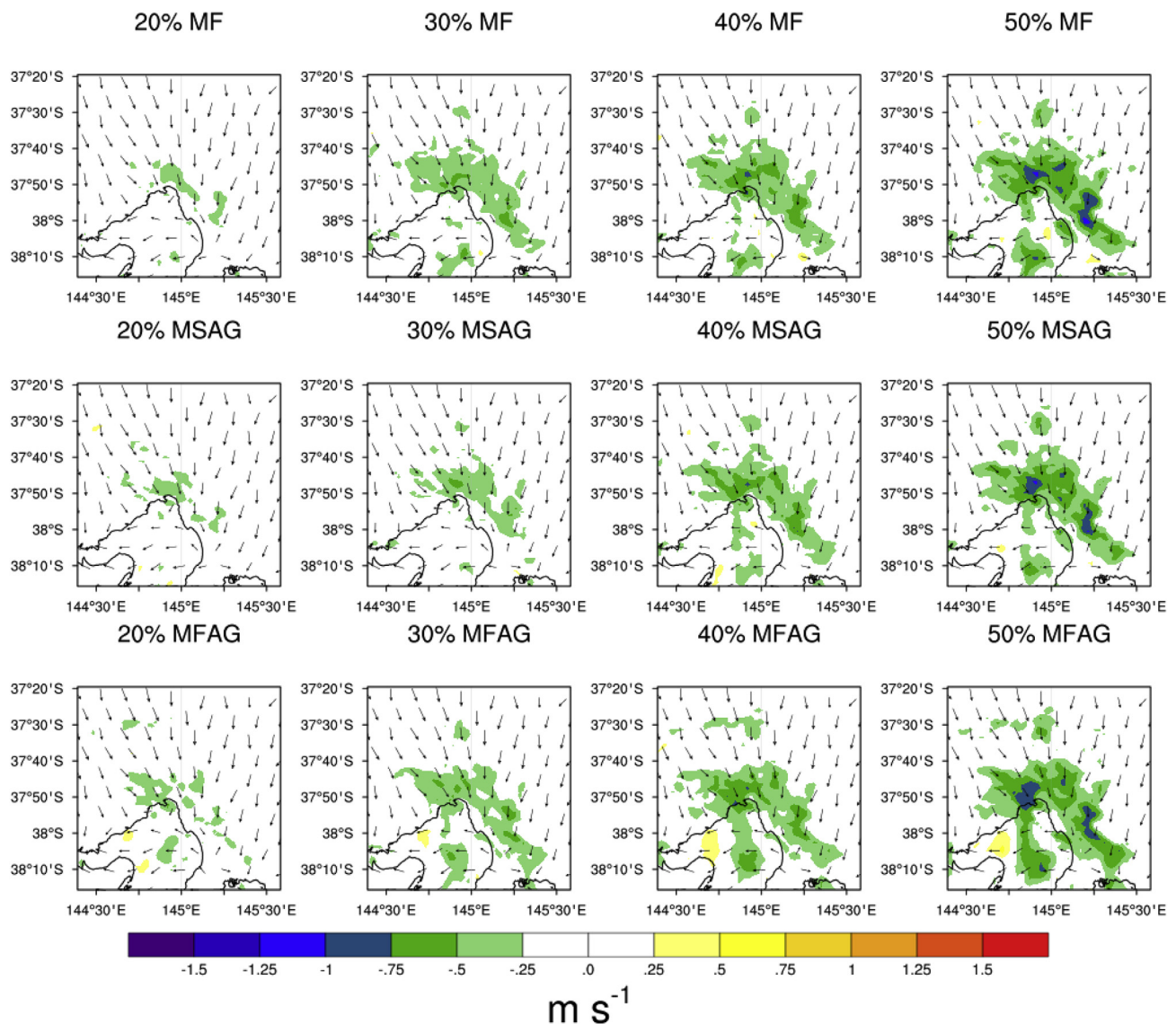
Fig. 9. Wind direction (only for experiments) and changes in wind speed (experiments minus control) for MF (upper), MSAG (middle) and MFAG (bottom) by using their fractions 20%, 30%, 40% and 50%. All results are averaged from 2100 to 0400 local time for the 3 days (28–30 January 2009) when maximum UHI$_2$ reductions occurred.

patches in reducing UHI effects was not substantial during the day as there were no changes in sensible heat flux. In addition, considerable reductions in wind speed were obtained for only 40 and 50% vegetated patches especially in the center of the city, and therefore, the cooling effects due to implementing vegetated patches stagnate in the center of the city. In addition, vegetated patches also improved HTC particularly during the night when substantial reductions of UHI occurred. Based on overall results, the findings of this study suggests that the urban greening strategy, released by the city of Melbourne to increase urban vegetation cover from 22 to 40% by 2040, could help to achieve a more thermally comfortable, sustainable and livable urban environment.

Finally, this study has some limitations that need to be discussed. Direct interactions between vegetation and urban surfaces are not accounted for in our model. In reality, shading effects of vegetation at the edges of vegetated patches on urban surfaces would likely result in even lower storage heat flux. Hence, the cooling effects reported in this study are likely to be under-estimated. The study quantified the effectiveness of different vegetated patches in mitigating UHI effects including future urban scenarios but without considering future warming which would be expected by 2050. Reductions in the UHI via vegetated patches could

be lower if there is substantial future warming. This study also assumed that vegetated patches are implemented within all urban grid cells rather than only within the future projected urban expansion area. It is unlikely that up to 40–50% vegetated patches can be practically implemented across the entire city. Hence, this study only provides estimates of the maximum possible benefits, rather than practical benefits considering the challenges of implementing vegetated patches at such large scales. It should also be noted that this study does not include anthropogenic heat emissions during the simulations, such as heat from air conditioning units.
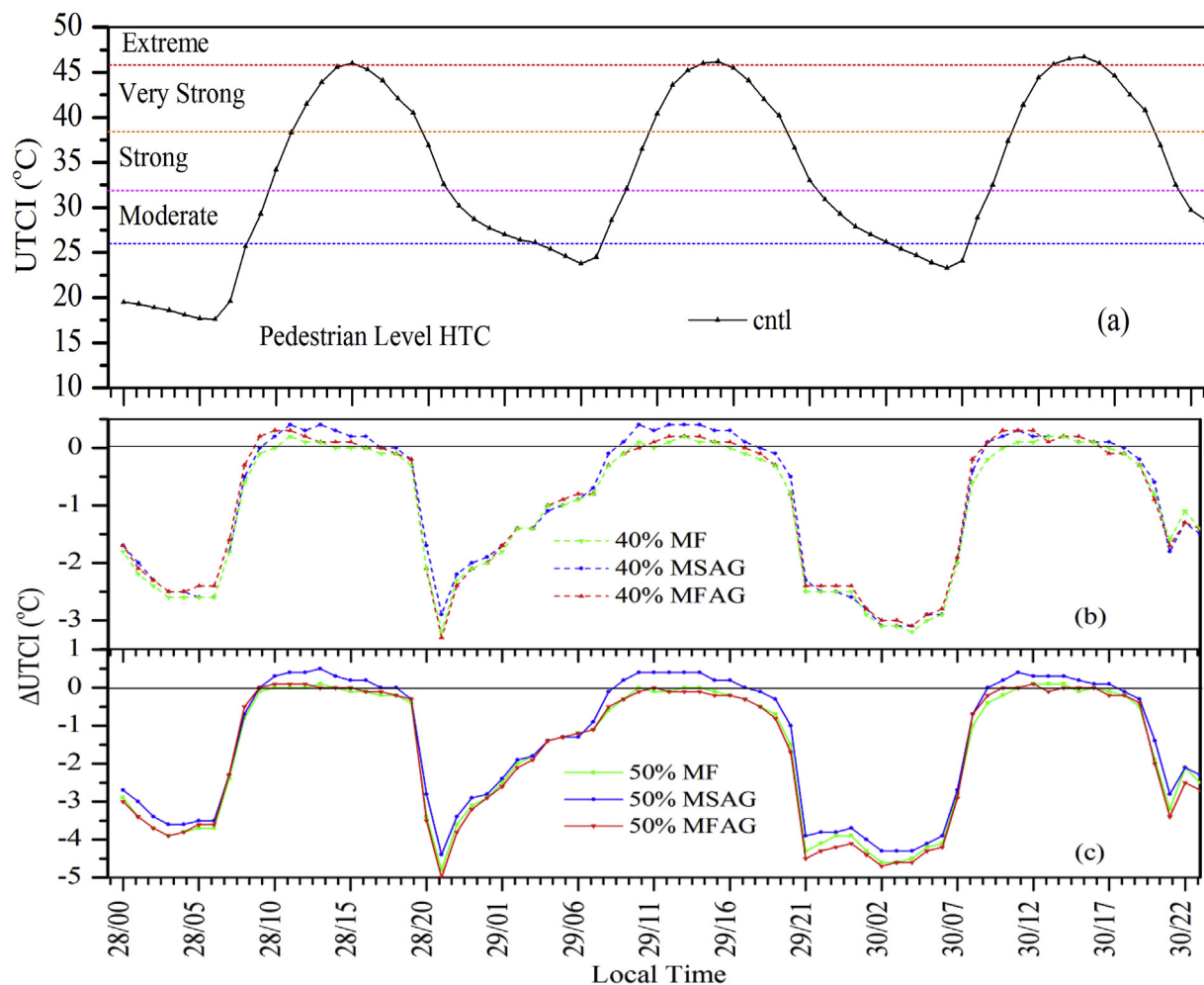
Acknowledgements

Fig. 10. (a) Hourly time series of the UTCI index at pedestrian level for the control simulation. (b) Changes in UTCI (experiment minus control) at pedestrian level for 40% and (c) 50% vegetated patches. All results are averaged over only urban grid cells across domain d03 for the 3 days from 28 to 30 January 2009.

Appendix A. Supplementary data

Supplementary data to this article can be found online at https://doi.org/10.1016/j.wace.2019.100217.

References

Akbari, H., Pomerantz, M., Taha, H., 2001. Cool surfaces and shade trees to reduce energy use and improve air quality in urban areas. Sol. Energy 70 (3), 295–310. https://doi.org/10.1016/S0038-092X(00)00089-X.

Ali-Toudert, F., Mayer, H., 2007. Effects of asymmetry, galleries, overhanging façades and vegetation on thermal comfort in urban street canyons. Sol. Energy 81 (6), 742–754. https://doi.org/10.1016/j.solener.2006.10.007.

Argüeso, D., Evans, J.P., Fita, L., Bormann, K.J., 2014. Temperature response to future urbanization and climate change. Clim. Dyn. 42 (7), 2183–2199. https://doi.org/10.1007/s00382-013-1789-6.

Australian Bureau of Statistics, 2008. ABS 3222.0 Population projections, Australia 2006 to 680 2101. viewed 7 August 2018: 681. http://www.abs.gov.au/Ausstats/abs@.nsf/Latestproducts/3222.0.

Blazejczyk, K., Epstein, Y., Jendritzky, G., Staiger, H., Tinz, B., 2012. Comparison of UTCI to selected thermal indices. Int. J. Biometeorol. 56 (3), 515–535. https://doi.org/10.1007/s00484-011-0453-2.

Bowler, D.E., Buyung-Ali, L., Knight, T.M., Pullin, A.S., 2010. Urban greening to cool towns and cities: a systematic review of the empirical evidence. Landsc. Urban Plan. 97 (3), 147–155. https://doi.org/10.1016/j.landurbplan.2010.05.006.

Bröde, P., Fiala, D., Błażejczyk, K., Holmér, I., Jendritzky, G., Kampmann, B., ... Havenith, G., 2012. Deriving the operational procedure for the universal thermal climate index (UTCI). Int. J. Biometeorol. 56 (3), 481–494. https://doi.org/10.1007/s00484-011-0454-1.

Chen, F., Dudhia, J., 2001. Coupling an advanced land surface–hydrology model with the penn state–NCAR MM5 modeling system. Part I: model implementation and sensitivity. Mon. Weather Rev. 129 (4), 569–585. https://doi.org/10.1175/1520-0493(2001)129<0569:caalsh>2.0.co;2.

Chen, F., Kusaka, H., Bornstein, R., Ching, J., Grimmond, C.S.B., Grossman-Clarke, S., ... Zhang, C., 2011. The integrated WRF/urban modelling system: development, evaluation, and applications to urban environmental problems. Int. J. Climatol. 31 (2), 273–288. https://doi.org/10.1002/joc.2158.

Coutts, A.M., White, E.C., Tapper, N.J., Beringer, J., Livesley, S.J., 2016. Temperature and human thermal comfort effects of street trees across three contrasting street canyon environments. Theor. Appl. Climatol. 124 (1), 55–68. https://doi.org/10.1007/s00704-015-1409-y.

Cowan, T., Purich, A., Perkins, S., Pezza, A., Boschat, G., Sadler, K., 2014. More frequent, longer, and hotter heat waves for Australia in the twenty-first century. J. Clim. 27 (15), 5851–5871. https://doi.org/10.1175/jcli-d-14-00092.1.

Dee, D., Uppala, S., Simmons, A., Berrisford, P., Poli, P., Kobayashi, S., ... Bauer, P., 2011. The ERA-Interim reanalysis: configuration and performance of the data assimilation system. QJ Roy. Meteor. Soc. 137, 553–597.

Evans, J.P., Ekström, M., Ji, F., 2012. Evaluating the performance of a WRF physics ensemble over South-East Australia. Clim. Dyn. 39 (6), 1241–1258. https://doi.org/10.1007/s00382-011-1244-5.

Fallmann, J., Emeis, S., Suppan, P., 2013. Mitigation of urban heat stress - a modelling case study for the area of Stuttgart. Erde 144 (3–4), 202–216. https://doi.org/10.12854/erde-144-15.

Foster, J., Lowe, A., Winkelman, S., 2011. The value of green infrastructure for urban climate adaptation. Cent. Clean. Air Policy 750, 1–52.

Grell, G.A., Dévényi, D., 2002. A generalized approach to parameterizing convection combining ensemble and data assimilation techniques. Geophys. Res. Lett. 29 (14). https://doi.org/10.1029/2002GL015311. 38-31-38-34.

Harlan, S.L., Brazel, A.J., Prashad, L., Stefanov, W.L., Larsen, L., 2006. Neighborhood microclimates and vulnerability to heat stress. Soc. Sci. Med. 63 (11), 2847–2863. https://doi.org/10.1016/j.socscimed.2006.07.030.

Hathway, E.A., Sharples, S., 2012. The interaction of rivers and urban form in mitigating the Urban Heat Island effect: a UK case study. Build. Environ. 58, 14–22. https://doi.org/10.1016/j.buildenv.2012.06.013.

Honjo, T., Takakura, T., 1990. Simulation of thermal effects of urban green areas on their surrounding areas. Energy Build. 15 (3), 443–446. https://doi.org/10.1016/0378-7788(90)90019-F.

Howard, L., 1833. The Climate of London, vols. I–III Harvey and Dorton, London.

Iacono, M.J., Delamere, J.S., Mlawer, E.J., Shephard, M.W., Clough, S.A., Collins, W.D., 2008. Radiative forcing by long-lived greenhouse gases: calculations with the AER radiative transfer models. J. Geophys. Res.: Atmosphere 113 (D13). https://doi.org/10.1029/2008JD009944.

Imran, H.M., Kala, J., Ng, A.W.M., Muthukumaran, S., 2018a. Effectiveness of green and cool roofs in mitigating urban heat island effects during a heatwave event in the city of Melbourne in southeast Australia. J. Clean. Prod. 197, 393–405. https://doi.org/10.1016/j.jclepro.2018.06.179.

Imran, H.M., Kala, J., Ng, A.W.M., Muthukumaran, S., 2018b. An evaluation of the performance of a WRF multi-physics ensemble for heatwave events over the city of Melbourne in southeast Australia. Clim. Dyn. 50 (7), 2553–2586. https://doi.org/10.1007/s00382-017-3758-y.

Imran, H.M., Kala, J., Ng, A.W.M., Muthukumaran, S., 2018c. Impacts of future urban expansion on urban heat island effects during heatwave events in the city of Melbourne in southeast Australia. Q. J. R. Meteorol. Soc submitted for publication.

Jacobs, S.J., Gallant, A.J., Tapper, N.J., 2017. The sensitivity of urban meteorology to soil moisture boundary conditions: a case study in Melbourne, Australia. J. Appl. Meteorol. Climatol. 56 (8), 2155–2172.

Jacobs, S.J., Gallant, A.J., Tapper, N.J., Li, D., 2018. Use of cool roofs and vegetation to mitigate urban heat and improve human thermal stress in Melbourne, Australia. J. Appl. Meteorol. Climatol. 0 (0). https://doi.org/10.1175/jamc-d-17-0243.1. null.

Janjic, Z., 1994. The step-mountain eta coordinate model: further developments of the convection, viscous sublayer, and turbulence closure schemes. 122 (5).

Kala, J., Andrys, J., Lyons, T.J., Foster, I.J., Evans, B.J., 2015a. Sensitivity of WRF to driving data and physics options on a seasonal time-scale for the southwest of Western Australia. Clim. Dyn. 44 (3), 633–659. https://doi.org/10.1007/s00382-014-2160-2.

Kala, J., Evans, J.P., Pitman, A.J., 2015b. Influence of antecedent soil moisture conditions on the synoptic meteorology of the Black Saturday bushfire event in southeast Australia. Q. J. R. Meteorol. Soc. 141 (693), 3118–3129. https://doi.org/10.1002/qj.2596.

Krayenhoff, E.,S., Christen, A., Martilli, A., Oke, T.R., 2013. A multi-layer radiation model for urban neighbourhoods with trees. Boundary-Layer Meteorol. 151, 139–178. https://doi.org/10.1007/s10546-013-9883-1.

Kumar, R., Kaushik, S., 2005. Performance evaluation of green roof and shading for thermal protection of buildings. Build. Environ. 40 (11), 1505–1511.

Kusaka, H., Kimura, F., 2004. Coupling a single-layer urban canopy model with a simple atmospheric model: impact on urban heat island simulation for an idealized case. J. Meteorol. Soc. Jpn. Ser. II 82 (1), 67–80. https://doi.org/10.2151/jmsj.82.67.

Kusaka, H., Kondo, H., Kikegawa, Y., Kimura, F., 2001. A simple single-layer urban canopy model for atmospheric models: comparison with multi-layer and slab models. Boundary-Layer Meteorol. 101 (3), 329–358. https://doi.org/10.1023/a:1019207923078.

Lee, S.H., Park, S.U., 2008. A vegetated urban canopy model for meteorological and environmental modelling. Boundary-Layer Meteorol. 126, 73–102. https://doi.org/10.1007/s10546-007-9221-6.

Lemonsu, A., Masson, V., Shashua-Bar, L., Erell, E., Pearlmutter, D., 2012. Inclusion of vegetation in the Town Energy Balance model for modelling urban green areas. Geosci. Model Dev. (GMD) 5, 1377–1393. https://doi.org/10.5194/gmd-5-1377-2012.

Li, D., Bou-Zeid, E., Oppenheimer, M., 2014. The effectiveness of cool and green roofs as urban heat island mitigation strategies. Environ. Res. Lett. 9 (5), 055002.

Li, D., Sun, T., Liu, M., Yang, L., Wang, L., Gao, Z., 2015. Contrasting responses of urban and rural surface energy budgets to heat waves explain synergies between urban heat islands and heat waves. Environ. Res. Lett. 10 (5), 054009.

Lin, B.-S., Lin, Y.-J., 2010. Cooling effect of shade trees with different characteristics in a subtropical urban park. Hortscience 45 (1), 83–86.

Liu, Y., Chen, F., Warner, T., Basara, J., 2006. Verification of a mesoscale data-assimilation and forecasting system for the Oklahoma city area during the joint urban 2003 field project. J. Appl. Meteorol. Climatol. 45 (7), 912–929. https://doi.org/10.1175/jam2383.1.

Liu, X., Tian, G., Feng, J., Ma, B., Wang, J., Kong, L., 2018. Modeling the warming impact of urban land expansion on hot weather using the weather Research and forecasting model: a case study of Beijing, China. Adv. Atmos. Sci. 35 (6), 723–736. https://doi.org/10.1007/s00376-017-7137-8.

Loughner, C.P., Allen, D.J., Zhang, D.-L., Pickering, K.E., Dickerson, R.R., Landry, L., 2012. Roles of urban tree canopy and buildings in urban heat island effects: parameterization and preliminary results. J. Appl. Meteorol. Climatol. 51 (10), 1775–1793. https://doi.org/10.1175/jamc-d-11-0228.1.

Matzarakis, A., Rutz, F., Mayer, H., 2007. Modelling radiation fluxes in simple and complex environments—application of the RayMan model. Int. J. Biometeorol. 51 (4), 323–334. https://doi.org/10.1007/s00484-006-0061-8.

Matzarakis, A., Rutz, F., Mayer, H., 2010. Modelling radiation fluxes in simple and complex environments: basics of the RayMan model. Int. J. Biometeorol. 54 (2), 131–139. https://doi.org/10.1007/s00484-009-0261-0.

McMahon, E.T., Benedict, M., 2000. Green infrastructure. Plan. Comm. J. 37 (4), 4–7.

Melbourne Vic Council, 2011. Urban Forest Strategy: Making a Great City Greener: 2012-2032. City of Melbourne, Australia. https://books.google.com.bd/books/about/Urban_Forest_Strategy.html?id=jo0PMwEACAAJ&redir_esc=y.

Middel, A., Häb, K., Brazel, A.J., Martin, C.A., Guhathakurta, S., 2014. Impact of urban form and design on mid-afternoon microclimate in Phoenix Local Climate Zones. Landsc. Urban Plan. 122, 16–28. https://doi.org/10.1016/j.landurbplan.2013.11.004.

Mirzaei, P.A., Haghighat, F., 2010. Approaches to study urban heat island – abilities and limitations. Build. Environ. 45 (10), 2192–2201. https://doi.org/10.1016/j.buildenv.2010.04.001.

Morris, K.I., Chan, A., Morris, K.J.K., Ooi, M.C.G., Oozeer, M.Y., Abakr, Y.A., Al-Qrimli, H.F., 2017. Impact of urbanization level on the interactions of urban area, the urban climate, and human thermal comfort. Appl. Geogr. 79, 50–72. https://doi.org/10.1016/j.apgeog.2016.12.007.

Nairn, J.R., Fawcett, R.G., 2013. Defining Heatwaves: Heatwave Defined as a Heat-Impact Event Servicing All Community and Business Sectors in Australia. Centre for Australian Weather and Climate Research.

Nicholls, N., Larsen, S., 2011. Impact of drought on temperature extremes in Melbourne, Australia. Aust. Meteorol. Oceanogr. J. 61 (2), 113–116.

Nicholls, N., Skinner, C., Loughnan, M., Tapper, N., 2008. A simple heat alert system for Melbourne, Australia. Int. J. Biometeorol. 52 (5), 375–384. https://doi.org/10.1007/s00484-007-0132-5.

Ohashi, Y., Genchi, Y., Kondo, H., Kikegawa, Y., Yoshikado, H., Hirano, Y., 2007. Influence of air-conditioning waste heat on air temperature in tokyo during summer: numerical experiments using an urban canopy model coupled with a building energy model. J. Appl. Meteorol. Climatol. 46 (1), 66–81. https://doi.org/10.1175/jam2441.1.

Oliveira, S., Andrade, H., Vaz, T., 2011. The cooling effect of green spaces as a contribution to the mitigation of urban heat: a case study in Lisbon. Build. Environ. 46 (11), 2186–2194. https://doi.org/10.1016/j.buildenv.2011.04.034.

Papangelis, G., Tombrou, M., Dandou, A., Kontos, T., 2012. An urban "green planning" approach utilizing the Weather Research and Forecasting (WRF) modeling system. A case study of Athens, Greece. Landsc. Urban Plan. 105 (1), 174–183. https://doi.org/10.1016/j.landurbplan.2011.12.014.

Park, M., Hagishima, A., Tanimoto, J., Narita, K.-i., 2012. Effect of urban vegetation on outdoor thermal environment: field measurement at a scale model site. Build. Environ. 56, 38–46. https://doi.org/10.1016/j.buildenv.2012.02.015.

Perkins-Kirkpatrick, S.E., White, C.J., Alexander, L.V., Argüeso, D., Boschat, G., Cowan, T., ... Purich, A., 2016. Natural hazards in Australia: heatwaves. Clim. Change 139 (1), 101–114. https://doi.org/10.1007/s10584-016-1650-0.

Redon, E.C., Lemonsu, A., Masson, V., Morille, B., Musy, M., 2017. Implementation of street trees within the solar radiative exchange parameterization of TEB in SURFEX v8.0. Geosci. Model Dev. (GMD) 10, 385–411. https://doi.org/10.5194/gmd-10-385-2017.

Rey, J.M., 1999. Modelling potential evapotranspiration of potential vegetation. Ecol. Model. 123 (2–3), 141–159.

Rizwan, A.M., Dennis, L.Y.C., Liu, C., 2008. A review on the generation, determination and mitigation of Urban Heat Island. J. Environ. Sci. 20 (1), 120–128. https://doi.org/10.1016/S1001-0742(08)60019-4.

Sharma, A., Conry, P., Fernando, H.J.S., Alan, F.H., Hellmann, J.J., Chen, F., 2016. Green and cool roofs to mitigate urban heat island effects in the Chicago metropolitan area: evaluation with a regional climate model. Environ. Res. Lett. 11 (6), 064004.

Sharma, A., Fernando, H.J.S., Hamlet, A.F., Hellmann, J.J., Barlage, M., Chen, F., 2017. Urban meteorological modeling using WRF: a sensitivity study. Int. J. Climatol. 37 (4), 1885–1900. https://doi.org/10.1002/joc.4819.

Shashua-Bar, L., Hoffman, M.E., 2000. Vegetation as a climatic component in the design of an urban street: an empirical model for predicting the cooling effect of urban green areas with trees. Energy Build. 31 (3), 221–235. https://doi.org/10.1016/S0378-7788(99)00018-3.

Shashua-Bar, L., Potchter, O., Bitan, A., Boltansky, D., Yaakov, Y., 2010. Microclimate modelling of street tree species effects within the varied urban morphology in the Mediterranean city of Tel Aviv, Israel. Int. J. Climatol. 30 (1), 44–57. https://doi.org/10.1002/joc.1869.

Skamarock, W., Klemp, J., Dudhia, J., Gill, D., Barker, D., Duda, M., ... Powers, J., 2008. A Description of the Advanced Research WRF Version 3. NCAR Technical Note. NCAR/TN\u2013475? STR, pp. 123.

Tanaka, K., Hashimoto, S., 2006. Plant canopy effects on soil thermal and hydrological properties and soil respiration. Ecol. Model. 196 (1–2), 32–44.

Theeuwes, N.E., Solcerová, A., Steeneveld, G.J., 2013. Modeling the influence of open water surfaces on the summertime temperature and thermal comfort in the city. J. Geophys. Res.: Atmosphere 118 (16), 8881–8896. https://doi.org/10.1002/jgrd.50704.

Thompson, G., Field, P.R., Rasmussen, R.M., Hall, W.D., 2008. Explicit forecasts of winter precipitation using an improved Bulk microphysics scheme. Part II: implementation of a new snow parameterization. Mon. Weather Rev. 136 (12), 5095–5115. https://doi.org/10.1175/2008mwr2387.1.

Vatani, J., Golbabaei, F., Dehghan, S.F., Yousefi, A., 2016. Applicability of Universal Thermal Climate Index (UTCI) in occupational heat stress assessment: a case study in brick industries. Ind. Health 54 (1), 14–19. https://doi.org/10.2486/indhealth.2015-0069.

Victorian Auditor General's Office, 2014. Heatwave management: reducing the risk to public health. Report tabled in State Parliament 14 October 2014. https://www.audit.vic.gov.au/sites/default/files/2017-07/20141014-Heatwave-Management.pdf.

Wang, Z.H., Bou-Zeid, E., Smith, J.A., 2013. A coupled energy transport and hydrological model for urban canopies evaluated using a wireless sensor network. Q. J. R. Meteorol. 920 Soc. 139, 1643–1657. https://doi.org/10.1002/Qj.2032.

Yu, C., Hien, W.N., 2006. Thermal benefits of city parks. Energy Build. 38 (2), 105–120. https://doi.org/10.1016/j.enbuild.2005.04.003.

Zhao, L., Oppenheimer, M., Zhu, Q., Baldwin, J.W., Ebi, K.L., Bou-Zeid, E., Liu, X., 2018. Interactions between urban heat islands and heat waves. Environ. Res. Lett. 13 (3), 034003.

Žuvela-Aloise, M., Koch, R., Buchholz, S., Früh, B., 2016. Modelling the potential of green and blue infrastructure to reduce urban heat load in the city of Vienna. Clim. Change 135 (3), 425–438. https://doi.org/10.1007/s10584-016-1596-2.